C66-6217

AEDC-TDR-63-186

[redacted]

[redacted]

FREE-OSCILLATION DYNAMIC STABILITY TESTS OF A 0.05-SCALE APOLLO COMMAND MODULE AND A 0.059-SCALE APOLLO LAUNCH ESCAPE VEHICLE AT SUPERSONIC SPEEDS

By

A. E. Hodapp, Jr.

von Kármán Gas Dynamics Facility

ARO, Inc.

a subsidiary of Sverdrup and Parcel, Inc.

[redacted]

[redacted]

ARO Project No. VT1244

NASA Offices and Research Centers Only

[redacted]

(This abstract is UNCLASSIFIED.)

ABSTRACT

Dynamic stability tests were conducted in the 40-Inch Supersonic Tunnel (A) of the von Kármán Gas Dynamics Facility on a 0.05-scale Apollo Command Module at Mach numbers 1.5 through 6 and on a 0.059-scale Apollo Launch Escape Vehicle at Mach numbers 1.5 through 4. Data were obtained at Reynolds numbers, based on maximum body diameter, ranging from 0.31×10^6 to 3.56×10^6 for the command module and 0.36×10^6 to 5.28×10^6 for the launch escape vehicle. The models were tested at model oscillation amplitudes of ±2 to ±15 deg for the command module and ±3 to ±12 deg for the launch escape vehicle. Selected test results are presented.

PUBLICATION REVIEW

This report has been reviewed and publication is approved.

Darreld K Calkins

Darreld K. Calkins
Major, USAF
AF Representative, VKF
DCS/Test

Jean A Jack

Jean A. Jack
Colonel, USAF
DCS/Test

PRECEDING PAGE BLANK NOT FILMED.

CONTENTS

ILLUSTRATIONS

NOMENCLATURE

A	Reference area (based on maximum model diam), ft^2
C_m	Pitching-moment coefficient, pitching moment/$q_\infty Ad$
C_{m_q}	$\partial C_m/\partial(qd/2V_\infty)$ } Damping-in-pitch derivatives, 1/rad
$C_{m_{\dot\alpha}}$	$\partial C_m/\partial(\dot\alpha d/2V_\infty)$ } Damping-in-pitch derivatives, 1/rad
C_{y_R}	Cycles to damp to a given amplitude ratio R, cycles
d	Reference length (maximum model diam), ft
f	Frequency of oscillation, cycles/sec
I	Model moment of inertia about the pivot axis, slug-ft^2
ℓ_n	Natural logarithm
M_∞	Free-stream Mach number
M_θ	Angular restoring moment parameter, ft-lb/rad
$M_{\dot\theta}$	Angular viscous damping moment parameter, $\frac{\text{ft-lb sec}}{\text{rad}}$
$M_{\dot\theta}'$	Aerodynamic angular viscous damping moment parameter, $\frac{\text{ft-lb sec}}{\text{rad}}$
q	Pitching velocity, rad/sec
q_∞	Free-stream dynamic pressure, lb/ft^2
R	Ratio of the amplitude of a damped oscillation after a given number of cycles to the initial amplitude
Re	Reynolds number based on maximum model diameter
t	Time, sec
V_∞	Free-stream velocity, ft/sec
α	Angle of attack, rad or deg
α_T	Trim angle, deg
$\dot\alpha$	Time rate of change of angle of attack, rad/sec
θ	Angular displacement from trim angle, rad or deg
$\dot\theta$	Angular velocity, rad/sec
$\ddot\theta$	Angular acceleration, rad/sec^2
ω	Angular frequency, rad/sec
$\omega d/2V_\infty$	Reduced frequency parameter, rad

SUBSCRIPTS

o	Maximum conditions
s	Structural conditions
w	Wind-on conditions

1.0 INTRODUCTION

At the request of the National Aeronautics and Space Administration Manned Spacecraft Center (NASA-MSC), dynamic stability tests were conducted at the von Kármán Gas Dynamics Facility (VKF), Arnold Engineering Development Center (AEDC), Air Force Systems Command (AFSC), for the North American Aviation Company (NAA). The purpose of these tests was to determine the effect of oscillation amplitude, Mach number, Reynolds number, cg position, and the addition of strakes on the aerodynamic damping characteristics of an Apollo Command Module (CM) Model and a Launch Escape Vehicle (LEV) Model at supersonic speeds.

The tests were conducted in the 40-Inch Supersonic Tunnel (A) during the period from April 18 through 25, 1963. Data were obtained with the 0.050-scale command module over a Mach number range of 1.5 through 6 at Reynolds numbers ranging from 0.31×10^6 to 3.56×10^6 and with the 0.059-scale launch escape vehicle over a Mach number range of 1.5 through 4 at Reynolds numbers ranging from 0.36×10^6 to 5.28×10^6. All Reynolds numbers are based on the maximum model body diameter. Data are presented in the form of the damping-in-pitch derivatives for the command module and launch escape vehicle at oscillation amplitudes (about the trim attitude) of ±2 to ±15 deg and ±3 to ±12 deg, respectively.

2.0 APPARATUS

2.1 WIND TUNNEL

The 40-Inch Supersonic Tunnel (A) (Fig. 1), is a continuous, closed circuit, variable density wind tunnel with an automatically driven, flexible-plate-type nozzle. The tunnel operates at Mach numbers from 1.5 to 6 at maximum stagnation pressures from 29 to 200 psia, respectively, and stagnation temperatures up to 300°F ($M_\infty = 6$). Minimum operating pressures are about one-tenth of the maximum at each Mach number. A complete description of the tunnel and airflow calibration information is given in Ref. 1.

2.2 DYNAMIC BALANCES

Two distinct balance systems were used in the present test program. Both were large amplitude (±20 deg) free oscillation systems; each was

Manuscript received August 1963.

equipped with a displacing-releasing mechanism which allowed the model to be released at any intermediate angle of attack. Angular transducers were used with each system and were of the variable reluctance type which provides a continuous time history of model displacement yet requires no physical connection between the moving and stationary parts of the balances. These transducers shown in Figs. 2 and 3 and described in detail in Ref. 2, produce an analog signal which is proportional to the angular displacement of the model.

The basic gas bearing balance system is shown in Fig. 2. The pivot used in this system (Fig. 4) is a cylindrical, gas journal bearing with inherent orifice compensation. A complete calibration of the load carrying ability and damping characteristics of this gas bearing can be found in Ref. 3.

The balance displacing mechanism as provided by NAA was operated manually. The model was positioned by the push-pull rods, the associated flex shafts, and the buckets on the model sector (Fig. 2). After the model was positioned at the desired angle of attack, it was locked in place by the brake and the flex shafts were retracted. After releasing the model, the brake could be used to arrest the model to re-engage the flex shafts.

The mechanical bearing balance system is shown in Fig. 3 and was designed and constructed by NAA. The pivot of this system was two instrument-type ball bearings which were each capable of withstanding a radial load of 250 lb. The model displacing mechanism consisted of three servomechanisms which made its operation completely automatic. Two of the servos were used to position and release the model while the third was used to arrest the model motion.

With the top slide plate in the most forward position, the bottom slide plate with associated rack gear could be driven forward or aft to position the model. This was accomplished through the contact of the rack gear, drive gear, and gear plate. A model release was obtained by activating a servo to move the top slide plate to its furthest aft position, thus disengaging the drive gear and gear plate. The third servo, which activated the cam, was used to arrest the model should it begin to diverge or to hold the model in position to re-engage the gears.

2.3 MODELS

The 0.05-scale Apollo Command Module (Fig. 5) and 0.059-scale Apollo Launch Escape Vehicle (Fig. 6) were designed and constructed by the North American Aviation Company. Both models were constructed of

aluminum and magnesium in an effort to minimize their moments of inertia. In addition, the models were designed so that the balance pivot axis could be located at various places in the model corresponding to expected cg positions of the full-scale vehicle. It was necessary to ballast these models for each pivot axis location so that the model center of gravity was placed at the pivot axis of the balance. Each model was designed with removable strakes which are shown in Fig. 7.

The 0.05-scale command module was designed to allow ±20 deg of motion about a nominal trim angle of 148 deg from the two cg positions as shown in Fig. 7. The 0.059-scale launch escape vehicle, shown in Fig. 8, was designed with an enlarged section near the apex of the command module, which was necessary to locate the balance pivot at the basic and centerline cg positions. With the balance at any of three cg positions, the LEV model could be oscillated ±20 deg about a nominal trim angle of zero.

Installation photographs of the command module and launch escape vehicle in the 40-Inch Supersonic Tunnel (A) are shown in Fig. 9.

3.0 PROCEDURE

Existing damping-in-pitch data obtained for the command module and launch escape vehicle did not provide sufficient knowledge of the effect of oscillation amplitude on the damping-in-pitch derivatives of these vehicles. This test program was therefore initiated in an attempt to evaluate the effect of Mach number, Reynolds number, addition of strakes, cg position, and primarily the effect of amplitude of oscillation on the damping-in-pitch derivatives of the command module and launch escape vehicle.

A test program of this type necessitates large model oscillation amplitudes (±20 deg) and, in addition, requires that the true model motion be realized. The latter requirement was particularly true for the launch escape vehicle which had an unsymmetrical aerodynamic restoring moment. This requirement can be accomplished only if the non-aerodynamic effects on the model motion such as balance restoring moment and tare damping can be eliminated or minimized.

The free-oscillation technique employed allows the model to be "flown" free from any external restoring moment. The damped oscillatory motion resulting from this technique is most conducive to studying the characteristics of the aerodynamic damping.

Balance tare damping can be minimized or almost eliminated depending on the type pivot employed. A gas bearing is particularly desirable since its tare damping can be considered negligible (Ref. 3). This type pivot was used in the command module but could not be used in the launch escape vehicle because of the location of the pivot axis.

The equation of motion for a free-oscillation, one-degree-of-freedom system may be expressed as

$$I\ddot{\theta} - M_{\dot{\theta}}\dot{\theta} - M_{\theta}\theta = 0 \qquad (1)$$

The method for computing the dimensionless damping-in-pitch derivatives from the free-oscillation tests is indicated as follows:

$$\theta = \theta_o e^{-(-M_{\dot{\theta}}/2I)t} \sin \sqrt{-M_{\theta}/I}\, t$$

$$M_{\dot{\theta}} = \frac{2I f_n R}{C_{Y_R}}$$

$$M_{\dot{\theta}}' = M_{\dot{\theta}_w} - M_{\dot{\theta}_a}$$

$$C_{m_q} + C_{m_{\dot{\alpha}}} = M_{\dot{\theta}}' 2V_\infty / q_\infty A d^2$$

The above linear theory can be applied to a non-linear system, such as the systems encountered in the present tests, when the data are reduced over an amplitude range for which the motion can be approximated as being exponentially damped and where the frequency remains approximately constant.

The test procedure was to displace the model from its trim attitude to the desired angle of attack and release it. The resulting oscillatory signal provided by the aforementioned angular transducer was recorded on a direct writing oscillograph and on magnetic tape by a high speed digital converter. Data was reduced from the magnetic tape on an IBM 7070 computer by a free-oscillation data reduction program.

Tests of the command module were conducted at Mach numbers 1.5 through 6 and at Reynolds numbers ranging from 0.31×10^6 to 3.56×10^6 based on model base diameter. Tests of the launch escape vehicle were conducted at Mach numbers of 1.5 to 4.0 and at Reynolds numbers ranging from 0.36×10^6 to 5.28×10^6 based on model base diameter. Oscillation amplitudes for the command module and launch escape vehicle were ±2 to ±15 deg and ±3 to ±12 deg, respectively.

4.0 PRECISION OF MEASUREMENTS

The angular transducers for each balance were calibrated during bench tests both before and after each tunnel test period, and check calibrations were made periodically during the runs to determine if any changes in calibration factors had occurred. Transducer calibrations were obtained through the use of known displacements, and model displacement was known within ±0.5 percent of the maximum value of the range in which the parameter was calibrated.

The ball bearing balance used with the LEV model was calibrated to obtain values of ball bearing tare damping. This tare damping was found to vary with radial load, frequency of oscillation, and amplitude; therefore, to obtain values of aerodynamic damping for the launch escape vehicle, the tare damping values were corrected to the wind-on conditions before subtracting them from the total values. It was not necessary to correct command module data for tare damping because of the negligible level of the gas bearing damping.

Considering the above uncertainties in each system, the estimated maximum uncertainties in $C_{m_q} + C_{m_{\dot{\alpha}}}$ for the command module are ±0.12 and for the launch escape vehicle, ±0.50.

5.0 RESULTS AND DISCUSSION

The effect of Mach number, Reynolds number, oscillation amplitude, cg position, and the addition of strakes on the damping-in-pitch derivatives for the command module are shown in Figs. 10 through 12.

The oscillograph traces which described the oscillatory motion of the command module indicated that both the motion and the damping were symmetrical about the trim attitude. Variations in Mach number, Reynolds number, oscillation amplitude, and module configuration were found to have no significant effect on the damping-in-pitch derivatives except at Mach 1.5 where amplitude of oscillation and removal of the strakes had an effect on the level of the damping-in-pitch derivatives (Fig. 11).

Motion of the launch escape vehicle, unlike that of the command module, was unsymmetrical about the trim attitude and deviated greatly from the damped motion described by Eq. (1). The damping coefficient (M'_θ) varied with frequency and the oscillation amplitude and was unsymmetrical; i. e., the envelope curves of the positive and negative peaks had different

variations with time. Therefore, a data reduction procedure was developed so that values of damping could be obtained from the envelope curve of the positive and negative peaks independently.

The results illustrated in Figs. 13 through 16 indicate that an increase in Reynolds number was stabilizing and that at the higher Reynolds numbers, the launch escape vehicle was dynamically stable over the amplitude ranges tested. These data also indicate that amplitude of oscillation had an effect on the damping-in-pitch derivatives.

Results obtained at Mach numbers 1.5 through 4 for the basic cg configuration with strakes are presented in Fig. 13. These data show that limit cycles existed at the lower Reynolds numbers for all Mach numbers with the exception of Mach 2. A comparison of the data for Mach numbers where the magnitude of the Reynolds numbers is approximately the same indicates that the level of the damping derivatives increased with increasing Mach number.

Data obtained at Mach numbers 1.5 through 3 for the basic cg configuration without strakes are presented in Fig. 14. The Mach 1.5 and 2 results, which were obtained at approximately the same Reynolds number, indicate that the level of the damping-in-pitch derivatives increased with Mach number. A comparison of the data obtained for both configurations of the basic cg (Figs. 13 and 14) at the higher Reynolds numbers for Mach numbers 1.5 through 3 reveals that a slight increase in model damping was obtained by removing the strakes. In addition, the two sets of data indicate that for the lower Reynolds numbers at Mach 3, removing the strakes had no effect on the amplitude of the limit cycle.

Results obtained at Mach numbers 2, 3, and 4 for the alternate cg position are presented in Fig. 15. These data indicate that limit cycles existed for the lower Reynolds numbers at Mach 3 and 4. A comparison of these data with data obtained at the basic cg position at Mach numbers 2 and 3 indicates that at the higher Reynolds numbers, model damping decreased slightly as the cg was moved from the basic to the alternate position. This comparison also shows that for the lower Reynolds number at Mach 3, the amplitude of the limit cycle had increased at the alternate position.

Data obtained at Mach numbers 1.5 through 3 for the centerline cg position are presented in Fig. 16. These data show that the damping at Mach numbers 2 and 3 was unsymmetrical. One would expect the trim angle of this configuration to be zero since it has both a symmetrical shape and cg position; however, the trim angle at Mach 1.5 and 3 was a positive 0.96 and 2.16 deg, respectively. A comparison of these data and

that of the basic cg (Fig. 14) at Mach number 3 reveals that at the lower Reynolds number, the limit cycle was eliminated when the cg was moved from the basic to the centerline position.

6.0 CONCLUSIONS

Free-oscillation dynamic stability tests were conducted on a 0.05-scale Apollo Command Module at Mach numbers 1.5 through 6 and on a 0.059-scale Apollo Launch Escape Vehicle at Mach numbers 1.5 through 4. Data were obtained at Reynolds numbers, based on maximum body diameter, ranging from 0.31×10^6 to 3.56×10^6 for the command module and 0.36×10^6 to 5.28×10^6 for the launch escape vehicle. Conclusions based on these data, obtained at oscillation amplitudes about the trim angle of ±2 to ±15 deg for the command module and ±3 to ±12 deg for the launch escape vehicle, are as follows:

6.1 COMMAND MODULE

1. No significant effect on the damping-in-pitch derivatives of the command module was obtained from variations of Mach number, Reynolds number, oscillation amplitude, and module configuration except at Mach 1.5 where removing the strakes increased the damping-in-pitch derivatives at oscillation amplitudes above $\theta = \pm 2$ deg and caused model damping to increase with amplitude.
2. No instabilities existed for the command module, and furthermore, its aerodynamic damping and oscillatory motion were symmetrical.

6.2 LAUNCH ESCAPE VEHICLE

1. Both the oscillatory motion and the aerodynamic damping of the launch escape vehicle were unsymmetrical.
2. Amplitude of oscillation affected the level of the damping-in-pitch derivatives for the launch escape vehicle at all Mach numbers; however, this effect generally decreased with decreasing Mach number.
3. Increasing Reynolds number increased the level of the damping-in-pitch derivatives for all models tested. The launch escape vehicle was positively damped at the higher Reynolds numbers; however, limit cycles did exist at the lower Reynolds numbers and at the lower amplitudes of oscillation.

4. At the basic cg position, removing the strakes slightly increased the level of the aerodynamic damping for the launch escape vehicle at Mach numbers 1.5 through 3.

REFERENCES

1. Test Facilities Handbook, (5th Edition). "von Kármán Gas Dynamics Facility, Vol. 4." Arnold Engineering Development Center, July 1963.

2. Welsh, C. J., Ledford, R. L., Ward, L. K., and Rhudy, J. P. "Dynamic Stability Tests in Hypersonic Tunnels and at Large Model Amplitudes." AEDC-TR-59-24, December 1959.

3. Hodapp, A. E., Jr. "Evaluation of a Gas Bearing Pivot for a High Amplitude Dynamic Stability Balance." AEDC-TDR-62-221, December 1962.

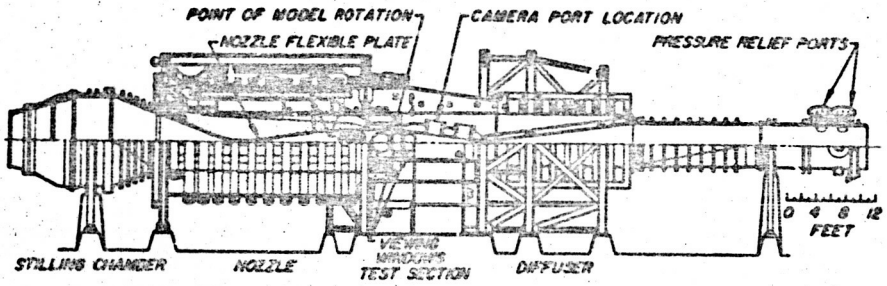

Assembly

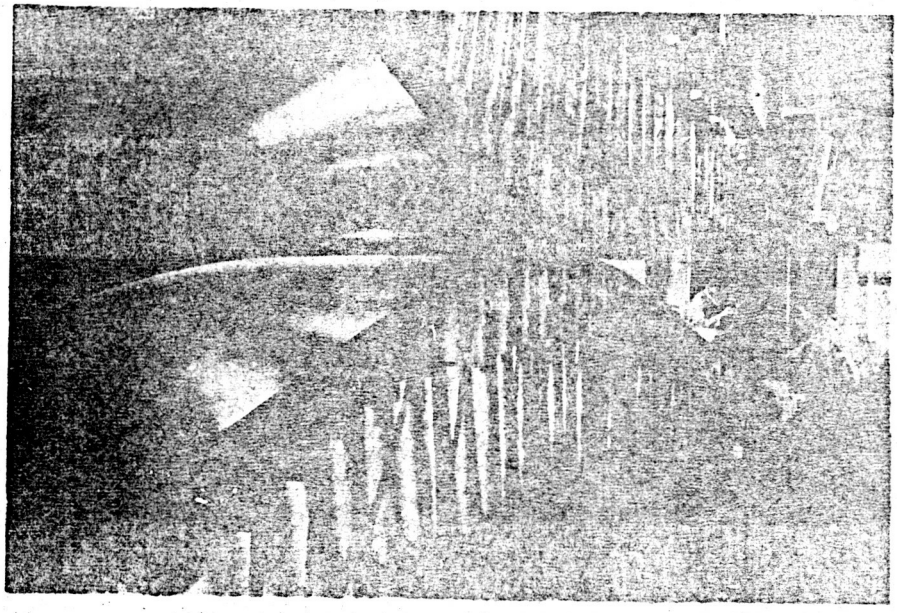

Nozzle and Test Section

Fig. 1 The 40-Inch Supersonic Tunnel (A)

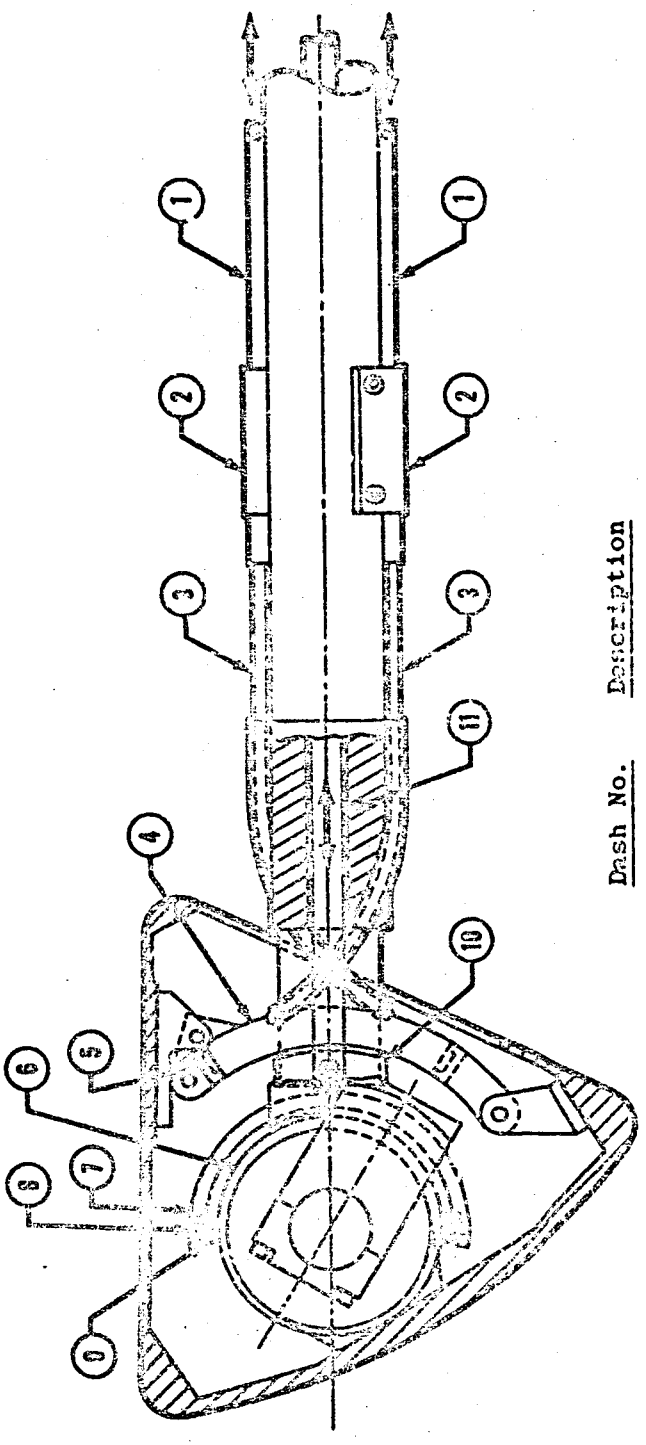

Dash No.	Description
1	Push Pull Rod
2	Rod Guide
3	Flex Shaft
4	Sector
5	Bucket
6	Eccentric
7	"E" Core Housing
8	"E" Core
9	Coil
10	Brake Shoe
11	Brake Rod

Fig. 2 Gas Bearing Balance Assembly

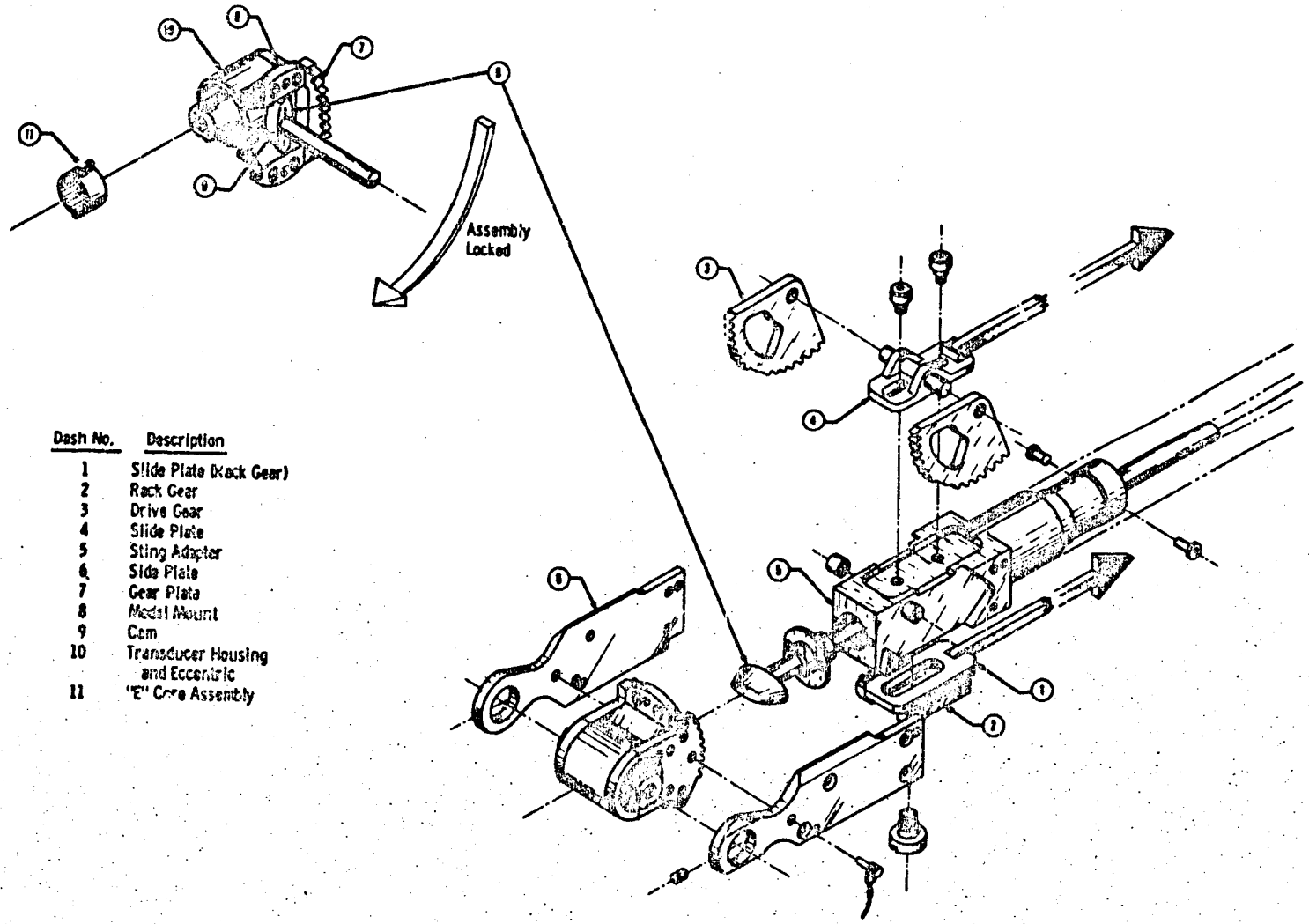

Dash No.	Description
1	Slide Plate (Rack Gear)
2	Rack Gear
3	Drive Gear
4	Slide Plate
5	Sting Adapter
6	Side Plate
7	Gear Plate
8	Model Mount
9	Cam
10	Transducer Housing and Eccentric
11	"E" Core Assembly

Fig. 3 Mechanical Bearing Balance Assembly

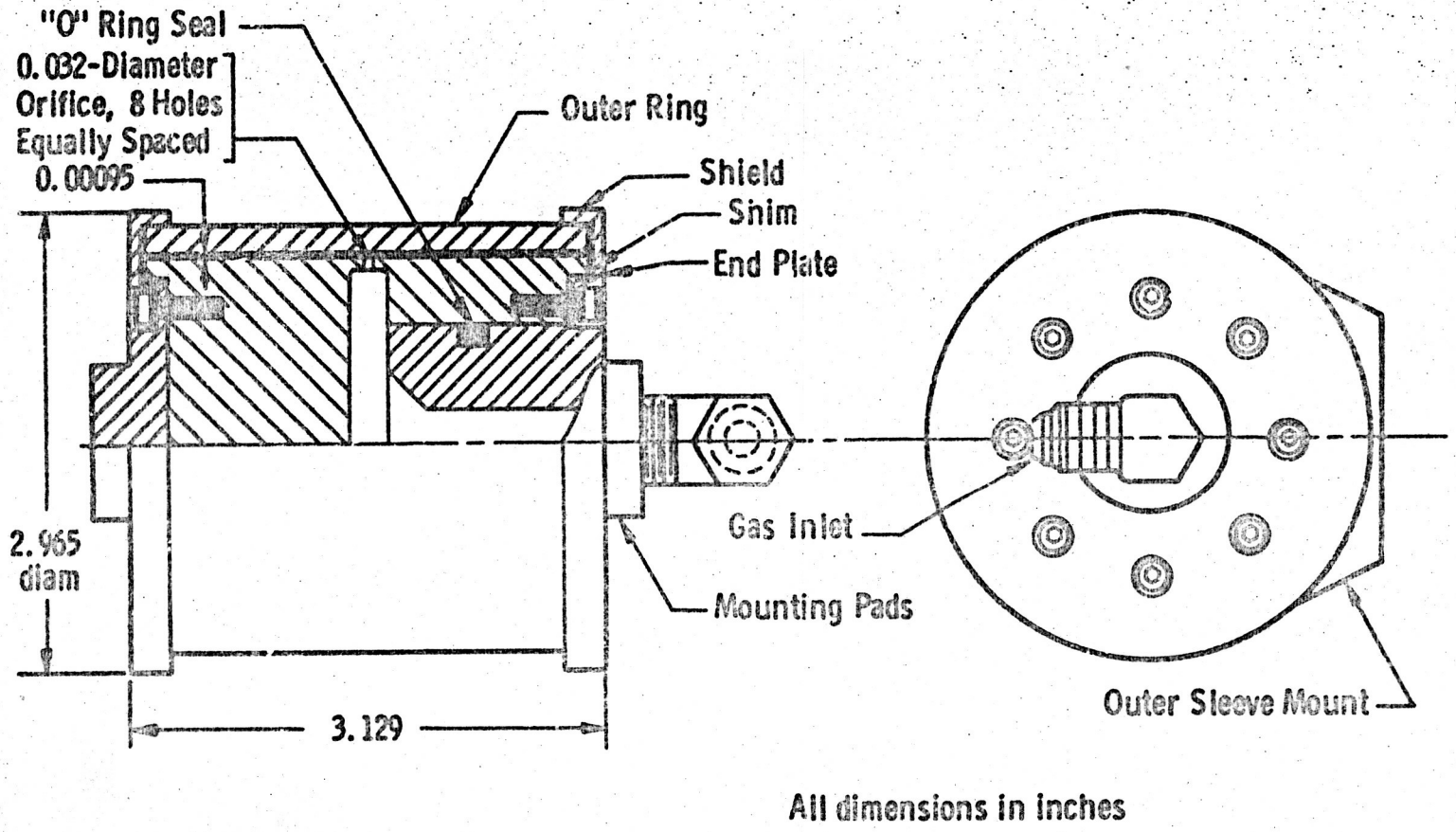

Fig. 4 Sketch of the Gas Bearing

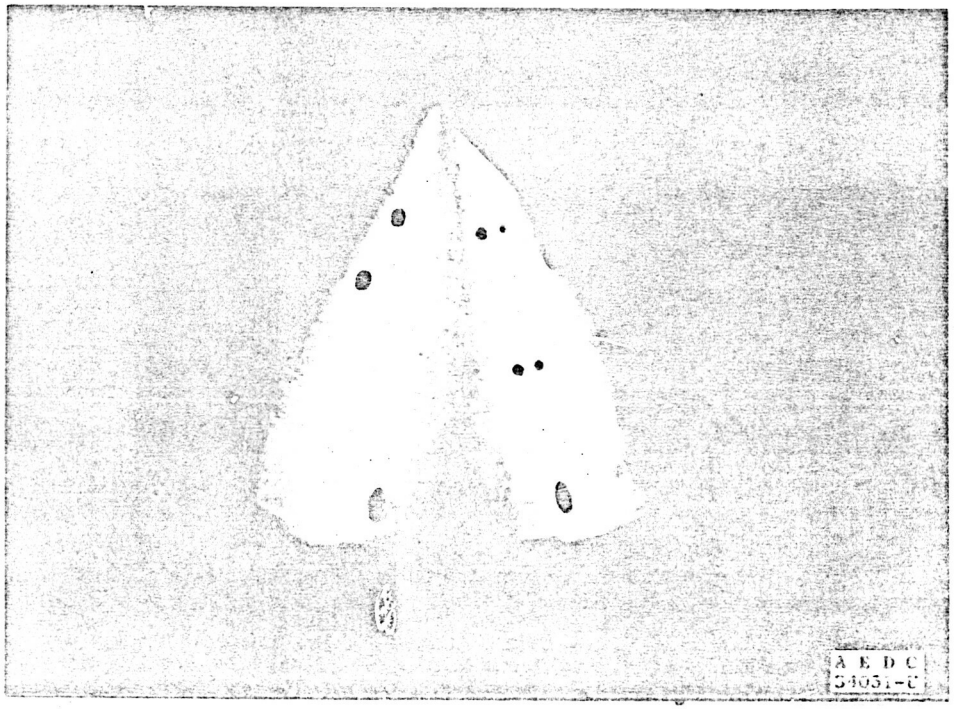

a. No Strakes

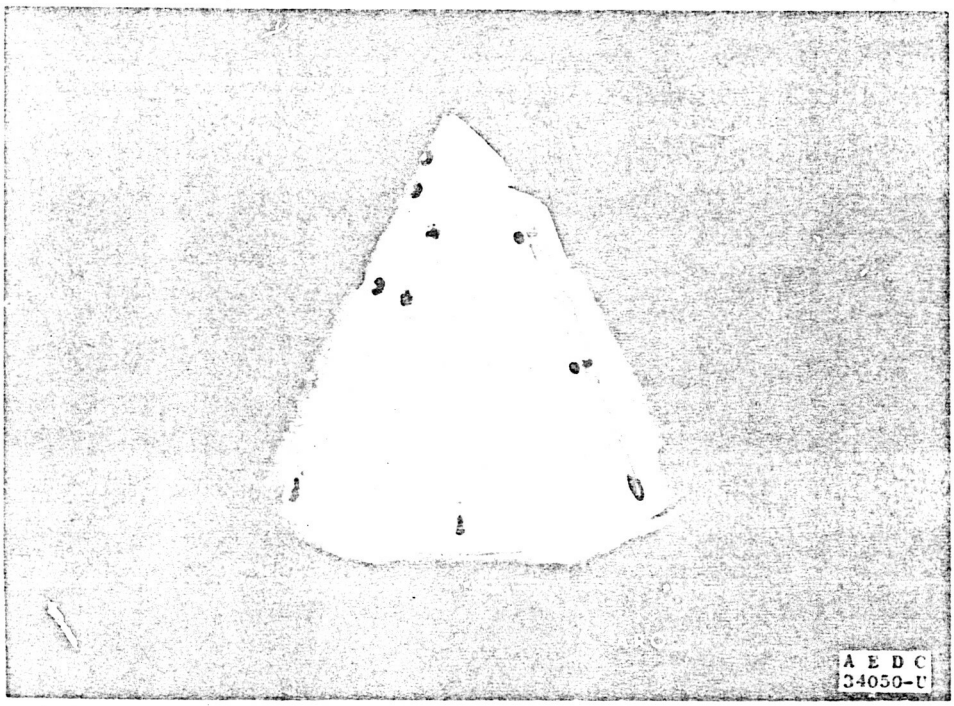

b. Strakes On

Fig. 5 Photograph of the 0.05-Scale Command Module

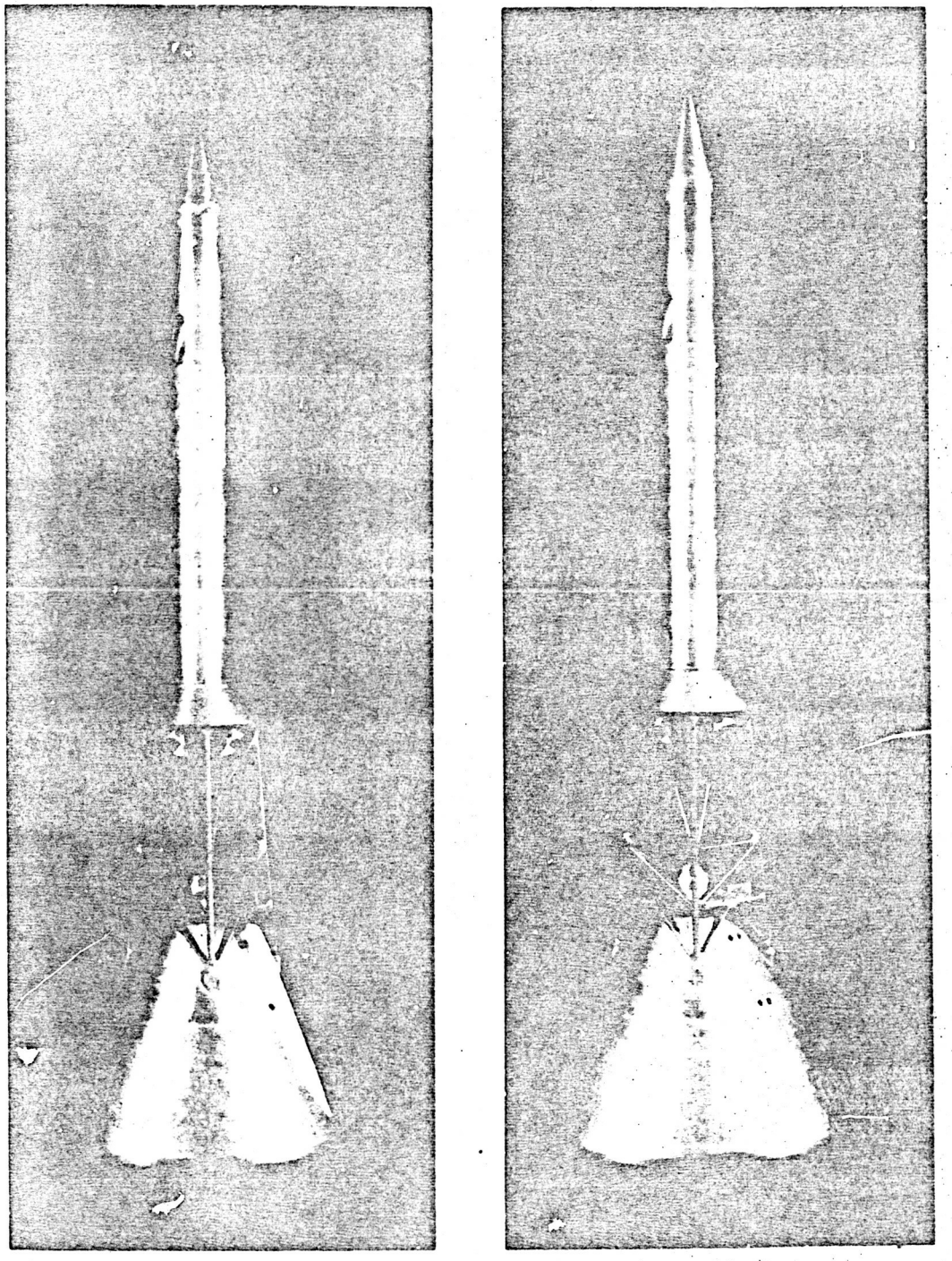

a. Strakes On

b. No Strakes

Fig. 6 Photograph of the 0.059-Scale Launch Escape Vehicle

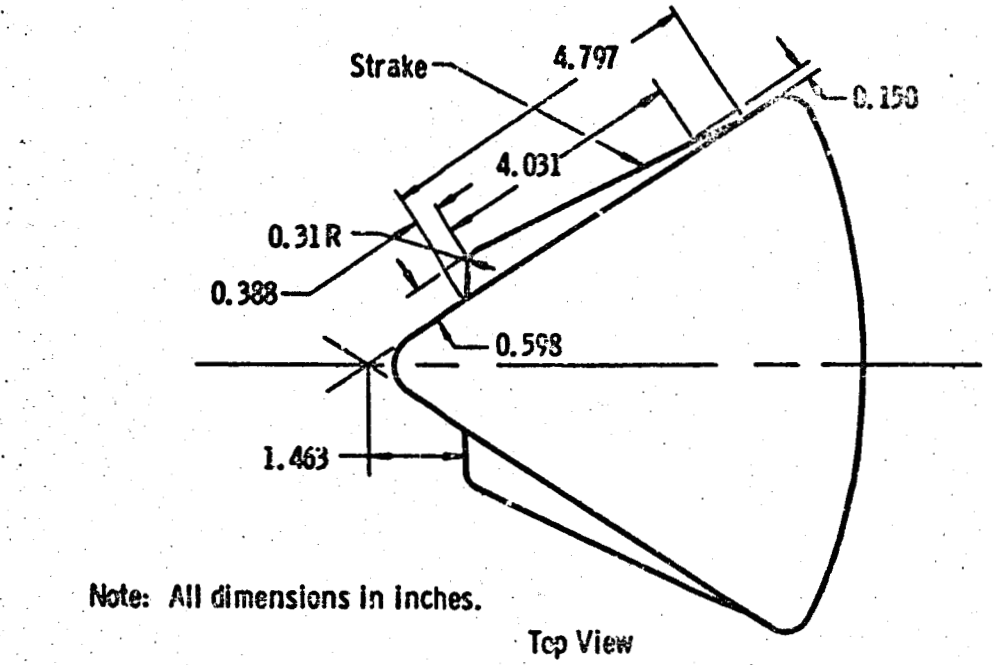

Note: All dimensions in inches.

Top View

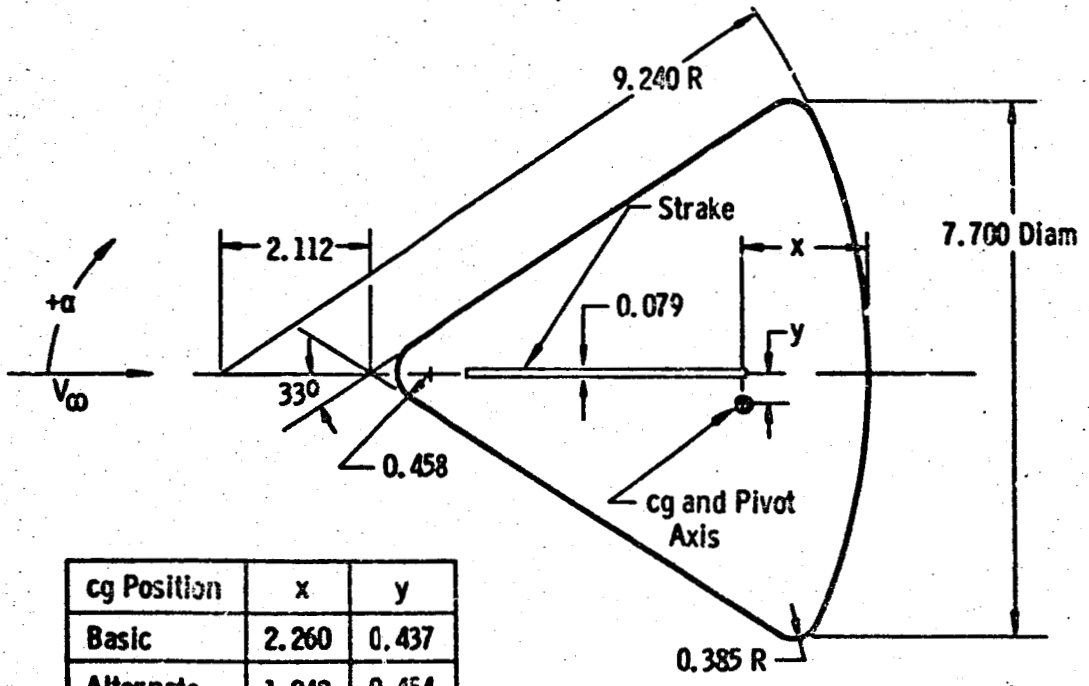

cg Position	x	y
Basic	2.260	0.437
Alternate	1.848	0.454

Side View

Fig. 7 Geometry of the 0.05-Scale Command Module

cg Position	x	y
Basic	6.520	0.336
Alternate	5.542	0.401
Centerline	6.520	0

Note: All dimensions in inches.

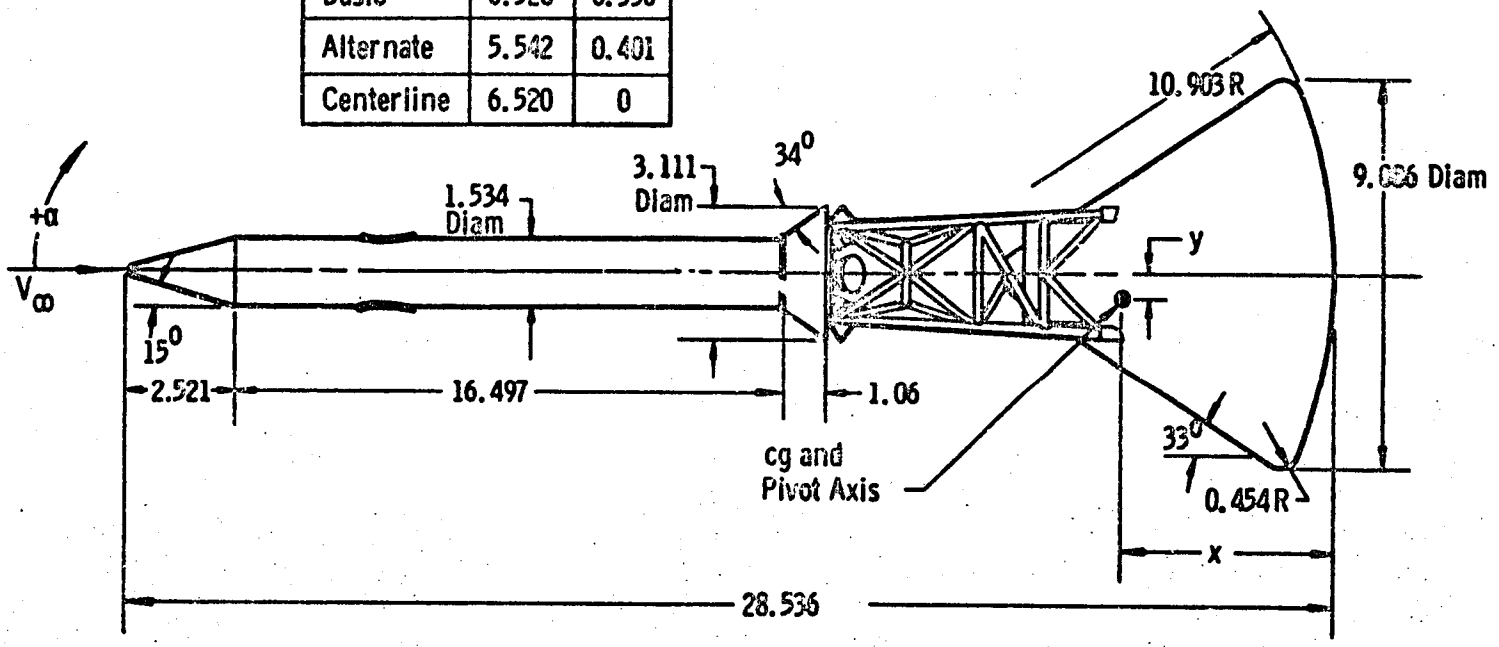

Fig. 8 Geometry of the 0.059-Scale Launch Escape Vehicle

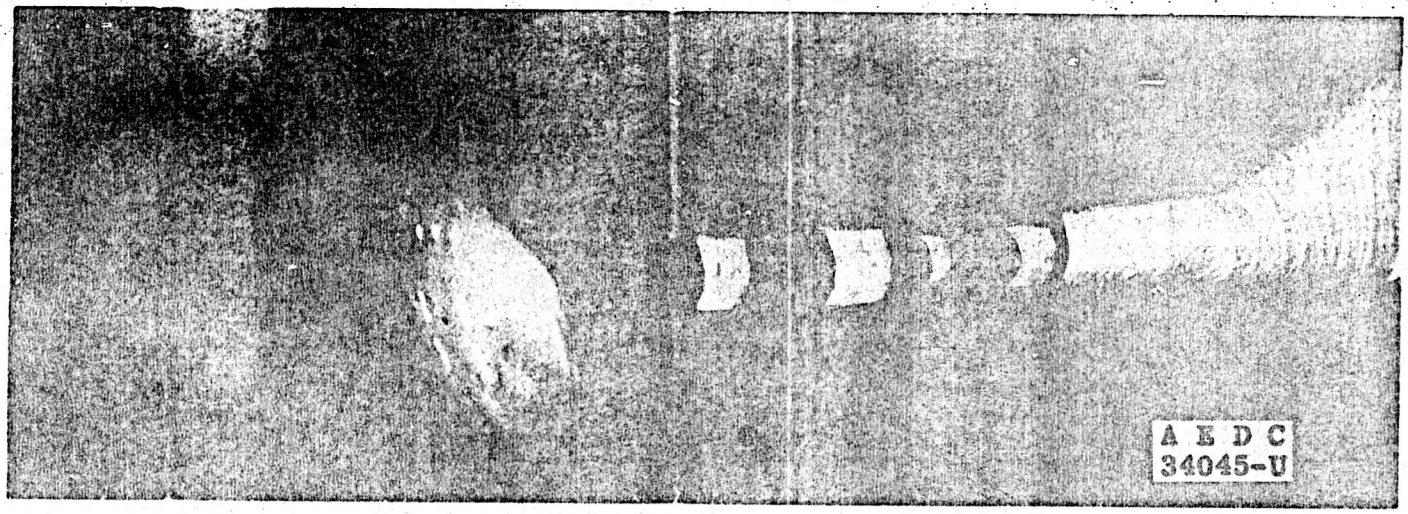

a. Command Module

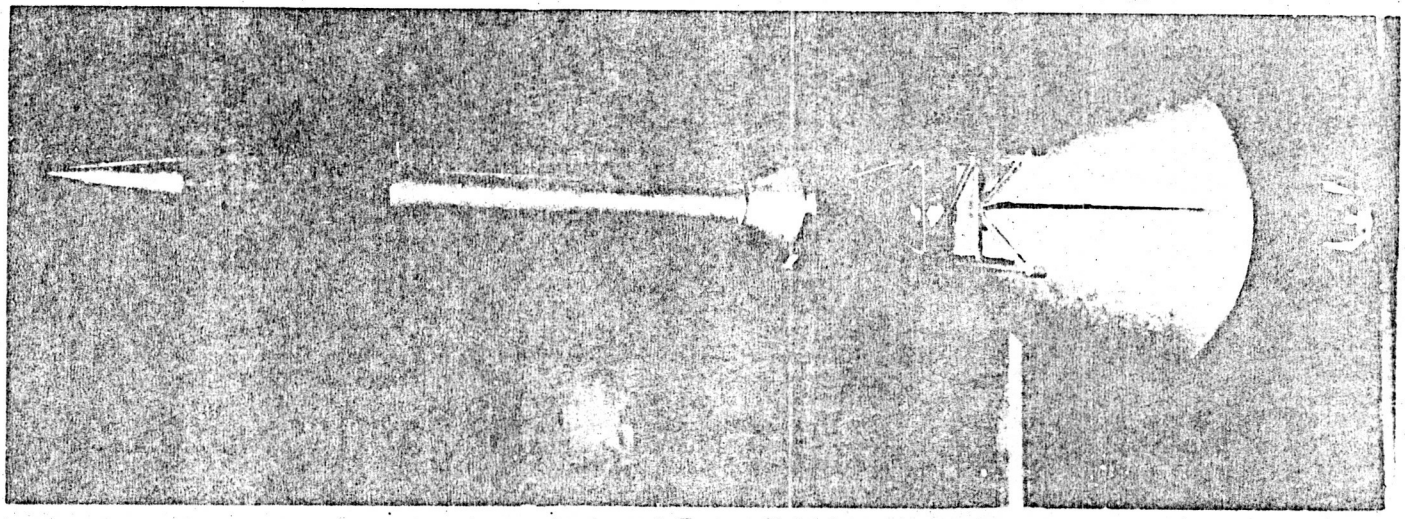

b. Launch Escape Vehicle

Fig. 9 Photograph of the Models Installed in the 40-inch Supersonic Tunnel (A)

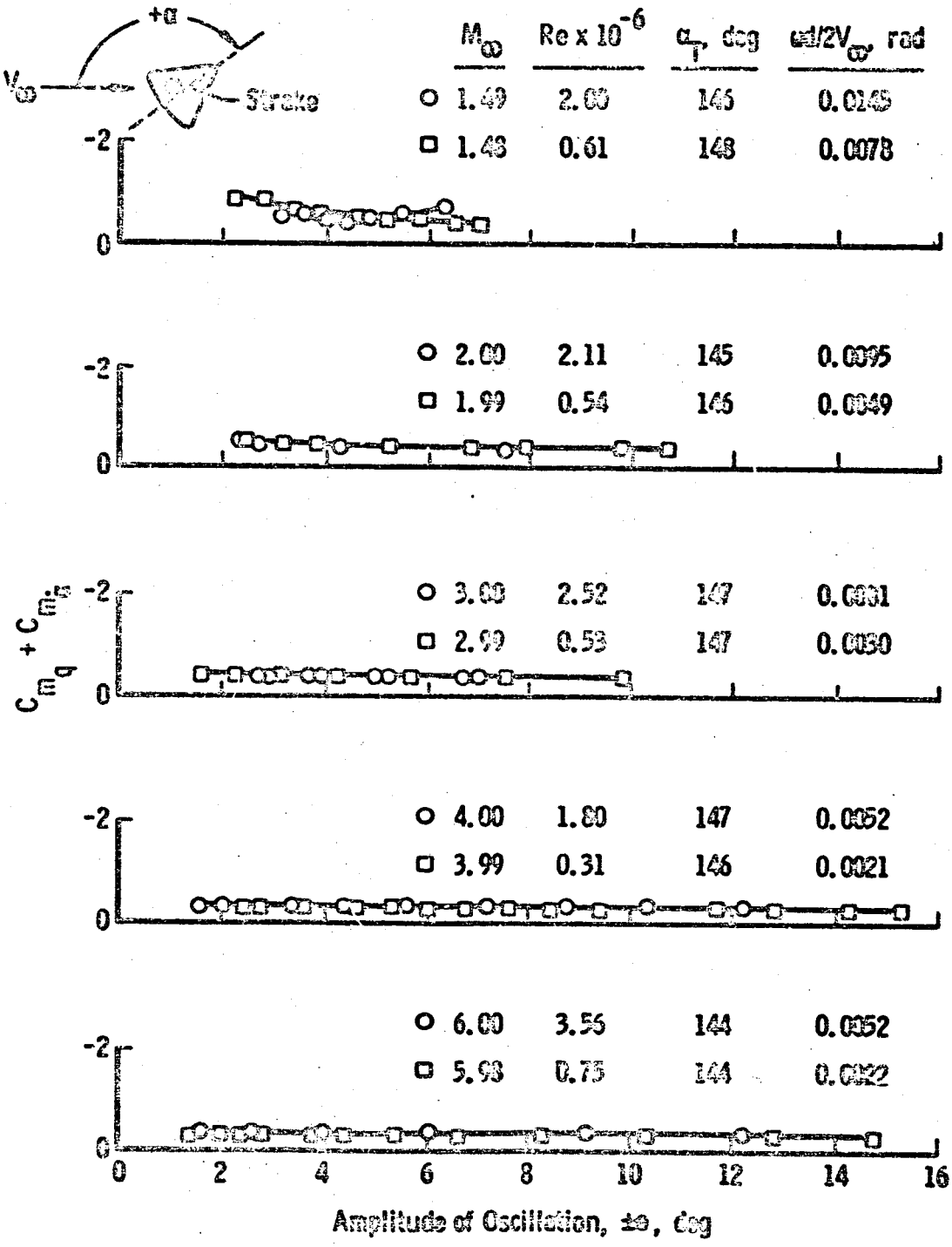

Fig. 10 Damping-in-Pitch Derivatives versus Amplitude of Oscillation about the Trim Attitude for the Command Module, Basic cg with Strakes

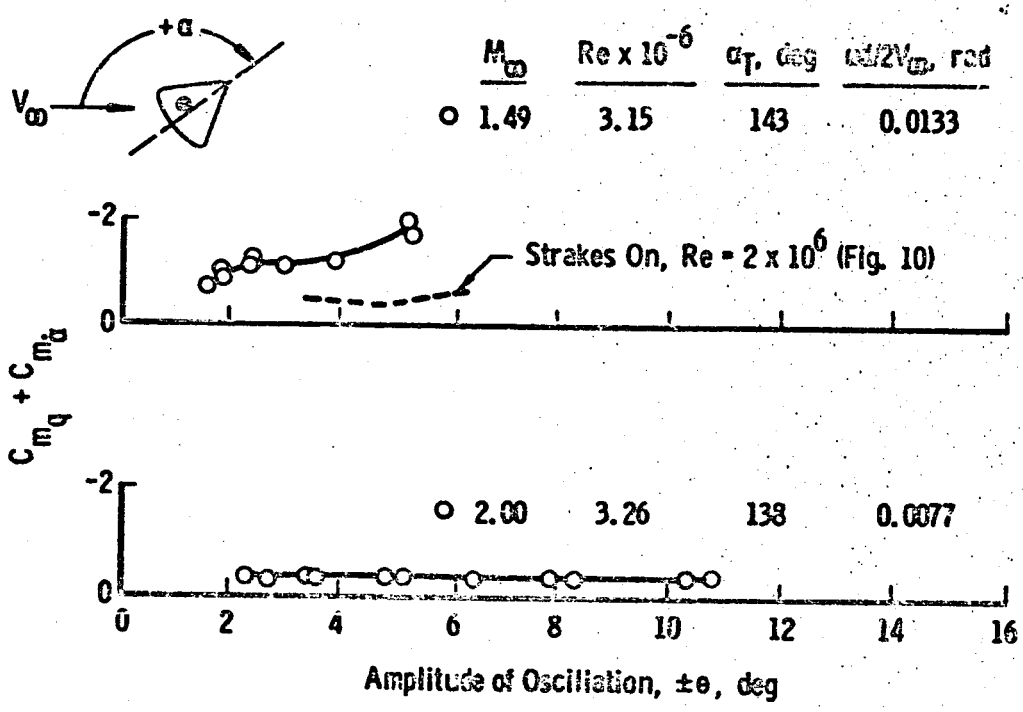

Fig. 11 Damping-in-Pitch Derivatives versus Amplitude of Oscillation about the Trim Attitude for the Command Module, Basic cg

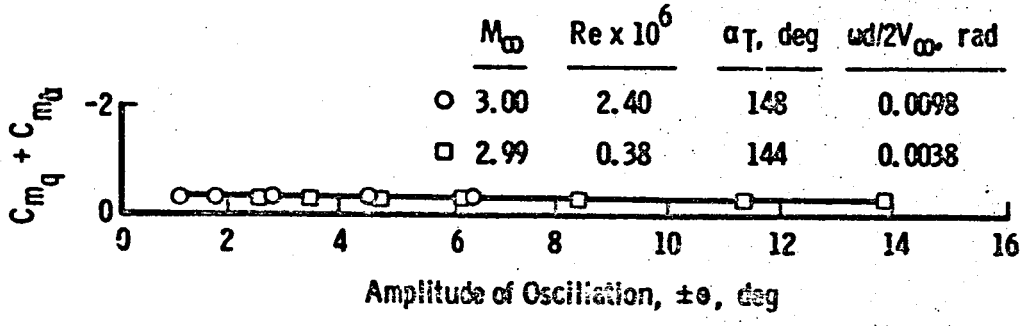

Fig. 12 Damping-in-Pitch Derivatives versus Amplitude of Oscillation about the Trim Attitude for the Command Module, Alternate cg

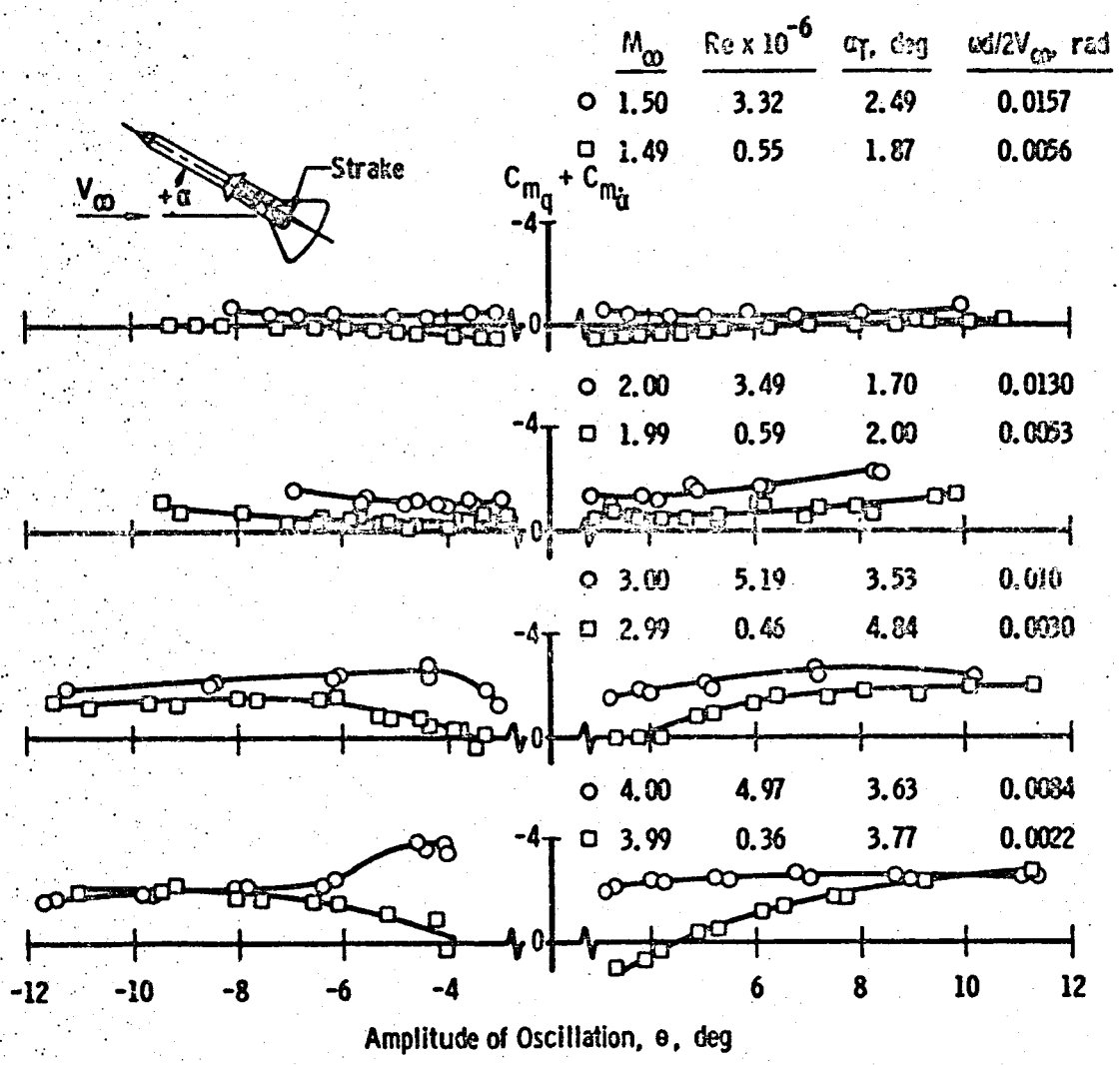

Fig. 13 Damping-in-Pitch Derivatives versus Amplitude of Oscillation about the Trim Attitude for the Launch Escape Vehicle, Basic cg with Strakes

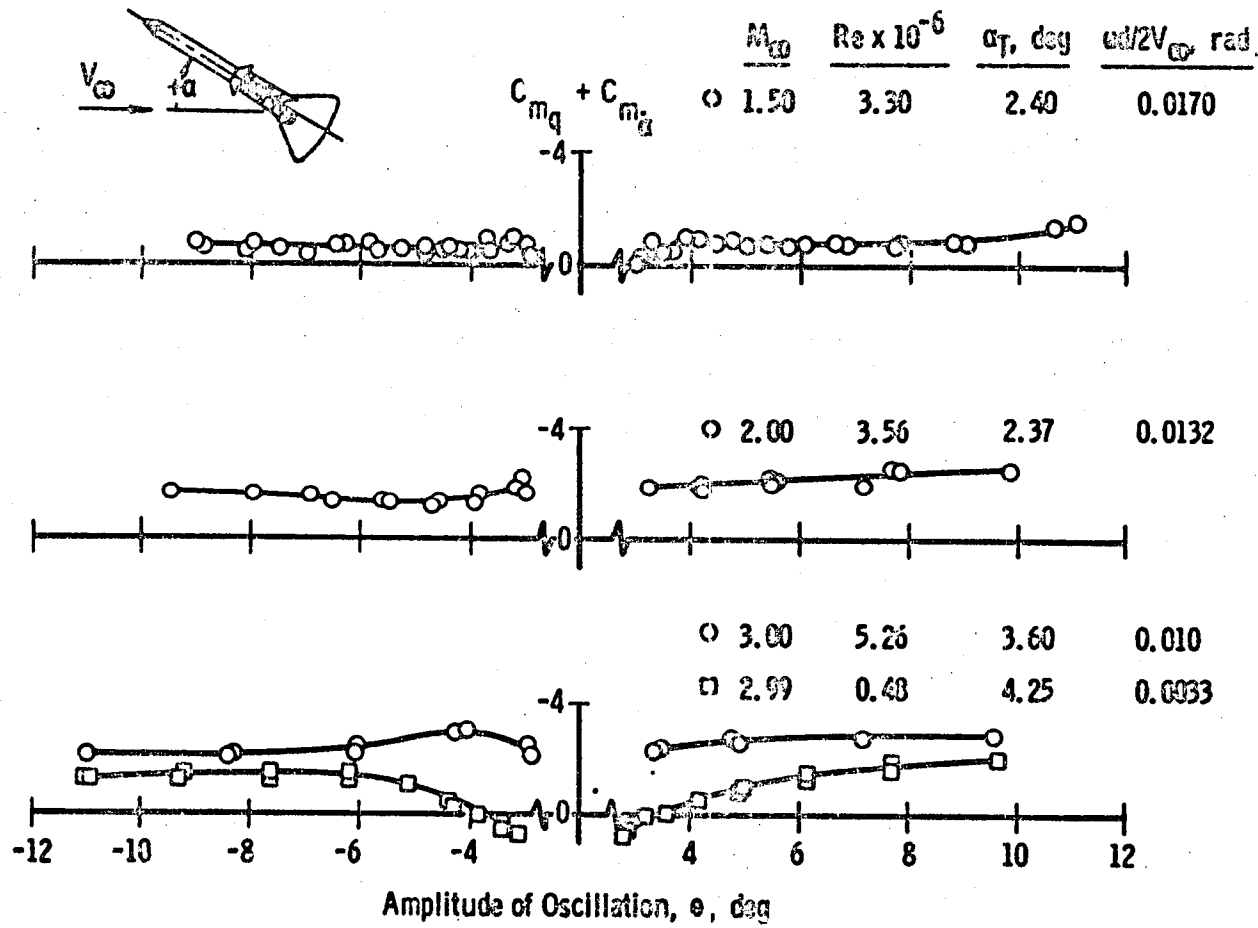

Fig. 14 Damping-in-Pitch Derivatives versus Amplitude of Oscillation about the Trim Attitude for the Launch Escape Vehicle, Basic cg

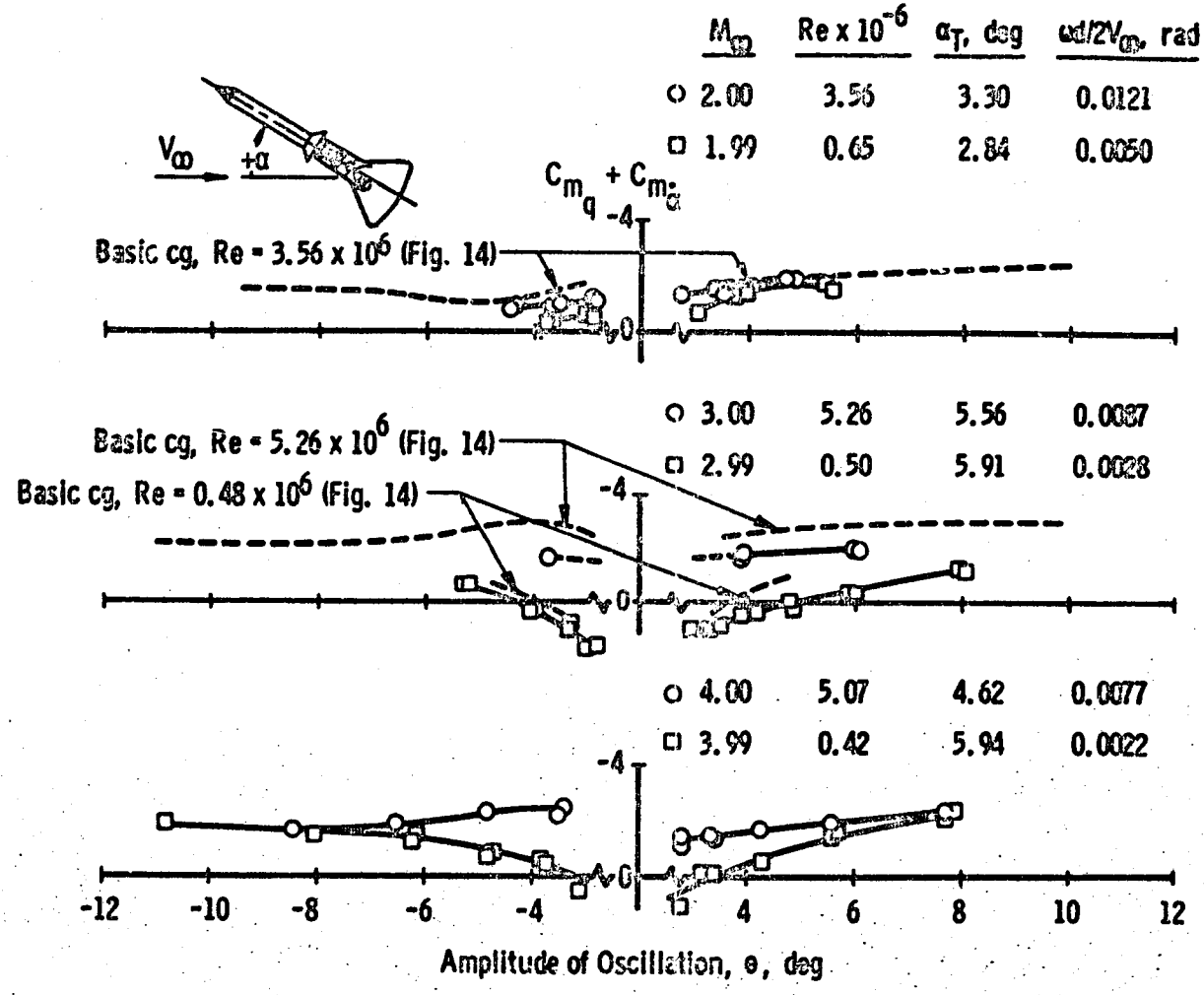

Fig. 15 Damping-in-Pitch Derivatives versus Amplitude of Oscillation about the Trim Attitude for the Launch Escape Vehicle, Alternate cg

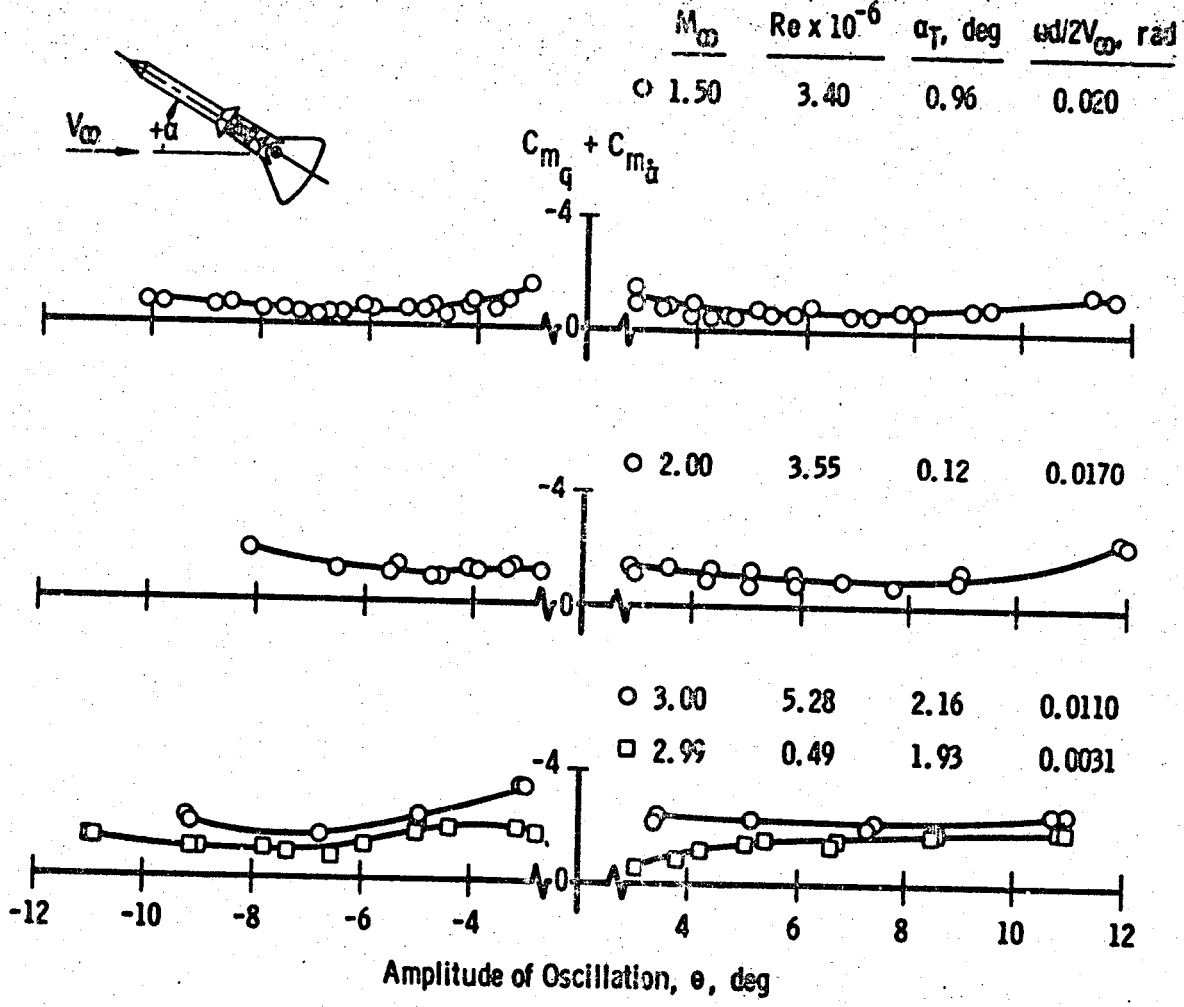

Fig. 16 Damping-in-Pitch Derivatives versus Amplitude of Oscillation about the Trim Attitude for the Launch Escape Vehicle, Centerline cg